Journal of Inorganic Biochemistry 219 (2021) 111408

Contents lists available at ScienceDirect

Journal of Inorganic Biochemistry

journal homepage: www.elsevier.com/locate/jinorgbio

Bioactive half-sandwich Rh and Ir bipyridyl complexes containing artemisinin

Prinessa Chellan [a,1], Vicky M. Avery [b], Sandra Duffy [b], Kirkwood M. Land [c], Christina C. Tam [d], Jong H. Kim [d], Luisa W. Cheng [d], Isolda Romero-Canelón [a], Peter J. Sadler [a,*]

[a] Department of Chemistry, University of Warwick, Coventry CV4 7AL, UK
[b] Discovery Biology, Griffith University, Nathan, Queensland 4111, Australia
[c] Department of Biological Sciences, University of the Pacific, Stockton, CA 95211, United States of America
[d] Foodborne Toxin Detection and Prevention Research Unit, Agricultural Research Service, United States Department of Agriculture, Albany, CA 94710, United States of America

ARTICLE INFO

Keywords:
Organometallic complexes
Antimicrobial
Anticancer
Rhodium
Iridium
Artemisinin

ABSTRACT

Reaction of dihydroartemisinin (**DHA**) with 4-methyl-4′-carboxy-2,2′-bipyridine yielded the new ester derivative **L1**. Six novel organometallic half-sandwich chlorido Rh(III) and Ir(III) complexes (**1–6**) containing pentamethylcyclopentadienyl, (Cp*), tetramethylphenylcyclopentadienyl (Cp^{xph}), or tetramethylbiphenylcyclopentadienyl (Cp^{xbiph}), and *N,N*-chelated bipyridyl group of **L1**, have been synthesized and characterized. The complexes were screened for inhibitory activity against the *Plasmodium falciparum* 3D7 (sensitive), Dd2 (multi-drug resistant) and NF54 late stage gametocytes (LSGNF54), the parasite strain *Trichomonas vaginalis* G3, as well as A2780 (human ovarian carcinoma), A549 (human alveolar adenocarcinoma), HCT116 (human colorectal carcinoma), MCF7 (human breast cancer) and PC3 (human prostate cancer) cancer cell lines. They show nanomolar antiplasmodial activity, outperforming chloroquine and artemisinin. Their activities were also comparable to dihydroartemisinin. As anticancer agents, several of the complexes showed high inhibitory effects, with Ir(III) complex **3**, containing the tetramethylbiphenylcyclopentadienyl ligand, having similar IC_{50} values (concentration for 50% of maximum inhibition of cell growth) as the clinical drug cisplatin (1.06–9.23 μM versus 0.24–7.2 μM, respectively). Overall, the iridium complexes (**1–3**) are more potent compared to the rhodium derivatives (**4–6**), and complex **3** emerges as the most promising candidate for future studies.

1. Introduction

Metal complexes have provided potential leads for the discovery of new medicines, especially for combatting antimicrobial and anticancer resistance [1–8]. The platinum drug, cisplatin, is widely used to treat a variety of cancers and its success has led to the development of other anticancer platinum complexes [9–12], and in turn to investigation of complexes containing other metals in the platinum group. Some ruthenium complexes have also recently reached clinical trials for cancer therapy [13–33] and rhodium, iridium and osmium complexes have shown high antiproliferative activities in various cancer cell lines and microbial pathogens further stimulating their development as antitumor and antiparasitic agents [34–42].

Artemisinin (ART) is a sesquiterpene lactone natural product extracted from the Chinese herb *qinghaosu*. The first report of its potential as an antimalarial agent was in 1979 [43] for which its discoverer, Youyou Tu, was awarded the 2015 Nobel Prize in Medicine [44]. ART is used today as part of the World Health Organisation's (WHO)

Abbreviations: ACT, artemisinin combination therapy; ART, artemisinin; ARS, artesunate; CDDP, cis-diamminedichloridoplatinum(II); Cp*, pentamethylcyclopentadienyl; Cp^{xph}, tetramethylphenylcyclopentadienyl; Cp^{xph}, tetramethylbiphenylcyclopentadienyl; CQ, chloroquine; DCM, dichloromethane; DHA, dihydroartemisinin; DMF, dimethylformamide; DMEM, Dulbecco's Modified Eagle Medium; DMSO, Dimethyl sulfoxide; DOXP, 1-deoxy-d-xylulose 5-phosphate; FBS, fetal bovine serum; HPLC, high performance liquid chromatography; HR-ESI-MS, high resolution-electrospray ionisation-mass spectrometry; IC_{50}, concentration for 50% of maximum inhibition of cell growth; RBC, red blood cell; ROS, reactive oxygen species; TFA, trifluoroacetic acid; WHO, World Health Organisation.

* Corresponding author.
E-mail address: p.j.sadler@warwick.ac.uk (P.J. Sadler).
[1] Current address: Stellenbosch University, Matieland, Western Cape, South Africa.

https://doi.org/10.1016/j.jinorgbio.2021.111408
Received 12 December 2020; Received in revised form 21 February 2021; Accepted 21 February 2021
Available online 3 March 2021
0162-0134/

recommended artemisinin combination therapy (ACT) for treatment of uncomplicated malaria [45].

ART and its analogues (Fig. 1) selectively target parasites because of their enhanced uptake by parasitized erythrocytes compared to healthy erythrocytes [46,47]. Studies have found that ART derivatives may exert their antiplasmodial activity through a multi-targeted approach. They target the more mature trophozoite stages of *Plasmodium falciparum*; ARTs are also hyperactive against the early ring stages of the intra-erythrocytic life cycle stages as well as the trophozoite forms. ARTs block the parasite from advancing to the mature stage by killing the ring stage forms, increasing the rigidity of the host red blood cell (RBC) priming them to be removed from the circulation by the spleen [48,49]. Within the acidic food vacoule of the plasmodium parasite, ART forms adducts with the free haem that is produced as a byproduct of haemoglobin digestion [50]. These ART-haem adducts can inhibit haemozoin polymerisation thus promoting accumulation of toxic haem [50]. ART derivatives are capable of alkylating parasite proteins [50] and may also generate reactive oxygen species (ROS) through a multistep process which likely involves cleavage of the endoperoxide bridge by endogenous iron (from haem) [51,52]. Altogether, these events cause oxidative stress, thus inducing parasite death [46,53,54]. Additionally, ART derivatives are able to block transmission of gametocytes to the *Anopheles* mosquito by direct killing of gametocytes and inhibition of gametocyte formation as a result of reduction of the asexual parasite population [55].

The ability of ART to generate ROS has logically led to its study as a cancer treatment with results showing that it can promote apoptosis, induce cell cycle arrest or block tumour cell growth, invasion and metastasis [56–58]. ART can readily be derivatised, for example by modification or replacement of its lactone group, allowing generation of numerous compound libraries with anticancer and/or antiplasmodial activity [59–64]. Some of these compounds include ferrocenyl derivatives, inspired by the successful incorporation of ferrocene into the antimalarial drug chloroquine (ferroquine) [65–68]. While ferroquine (FQ) has a similar mode of action as chloroquine (CQ) [69], it can also accumulate in the digestive food vacuole of resistant malaria parasites that carry the *P. falciparum* chloroquine resistant transporter (*Pf*CRT). The ferrocene moiety in ferroquine is also proposed to affect the redox potential within the parasite through increased generation of hydroxyl radicals in the cytosol which leads to oxidative stress [70]. The complexes known collectively as ferrocifens are another important example. These ferrocenyl derivatives are selective estrogen receptor modulators (SERMs) that are inhibitors of both MCF-7 (hormone dependent) and MDA-MB-231 (hormone independent) breast cancer cells, unlike their organic precursor, hydroxytamoxifen, which is active only against the MCF-7 cell line [71].

Reiter *et al.* showed that conjugation of ferrocene to ART via an ester linkage leads to a significant increase in antileukemic activity, compared to ART itself ($IC_{50} = 36.9\,\mu M$ (CCRF-CEM) and $26.9\,\mu M$ (CEM/ADR500)), in the human acute lymphoblastic CCRF-CEM (IC_{50} between 0.01 and $0.13\,\mu M$) and the multidrug resistant CEM/ADR5000 cell lines (IC_{50} between 0.53 and $8.20\,\mu M$) [72,73]. Linking two ART molecules to ferrocene had an even greater effect [72].

These reports demonstrate the potential of organometallic ART complexes as new therapeutics. Rhodium and iridium organometallic complexes that incorporate various key parasite pharmacophores have been reported with some examples showing increased activities compared to the metal-free analogues [74–79].

Thus, we have investigated the activity of cyclopentadienyl rhodium or iridium ART complexes (**1–6**) towards five human cancer cell lines. The ligand **L1** and its six complexes (**1–6**) were also screened on four protozoan parasite strains (three *P. falciparum* and one *T. vaginalis*), a healthy cell line and normal flora. To the best of our knowledge, this is the first report of Rh(III) or Ir(III) half-sandwich complexes containing the artemisininyl fragment. They were prepared by reaction of a bipyridyl artemisinin ligand **L1** with cyclopentadienyl rhodium(III) or iridium(III) dimers to yield novel complexes **1–6** (Scheme 1). Remarkably, as antiplasmodials, both the ligand and the complexes inhibited parasite growth at nanomolar concentrations and display higher or comparable *in vitro* anticancer activity to the clinical drug cisplatin.

2. Experimental

2.1. Chemicals and reagents

Rhodium trichloride trihydrate and iridium trichloride trihydrate were purchased from Precious Metals Online (PMO Pty Ltd). All reagent solvents to undertake the chemistry were obtained from Fisher Scientific and Sigma-Aldrich. Artemisinin and 4-methyl-4′-carboxy-2,2′-bipyridine were purchased from Carbosynth Limited. 1,2,3,4,5-Pentamethylcyclopentadiene was purchased from Sigma-Aldrich. Deuterated solvents (acetone-d_6, $CDCl_3$, MeOD-d_4) were purchased from Cambridge Isotopes Limited. All reagents and chemicals were used as received. Dihydroartemisinin [80], 2,3,4,5-tetramethylcyclopentadienyl-1,1′-biphenyl [81] and 2,3,4,5-tetramethylcyclopentadienylbenzene [82] were prepared according to literature procedures. Dichloro

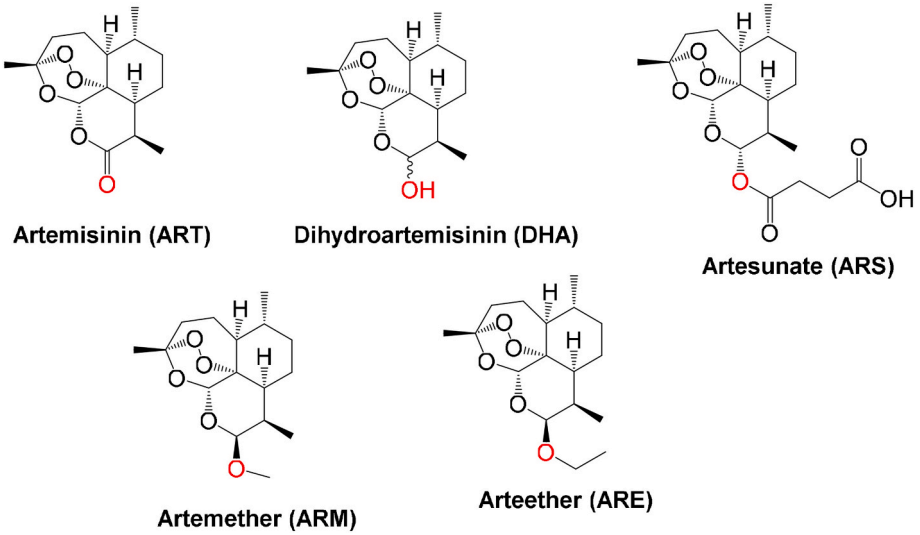

Fig. 1. Artemisinin (ART) and some of its analogues used in ACT treatment of malaria.

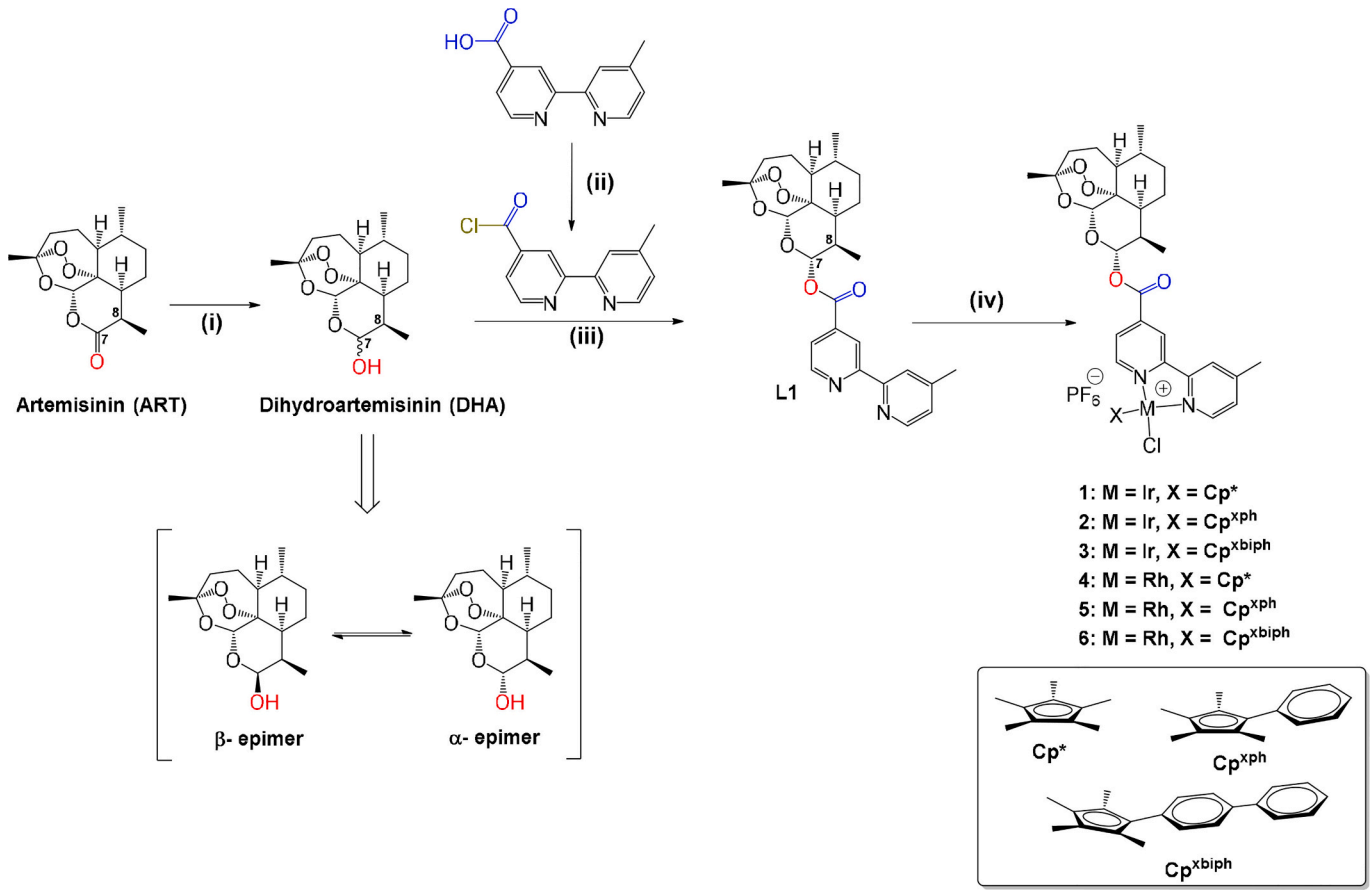

Scheme 1. Synthesis of **L1** and complexes **1–6**. (i) $NaBH_4$/MeOH; (ii) oxalyl chloride, Et_2O/cat. 3–4 drops DMF/0°-RT/18 h; (iii) DCM/Et_3N/5 h; (iv) $[XMCl_2]_2$/NH_4PF_6/DCM-MeOH/RT/18 h.

(pentamethylcyclopentadienyl)rhodium(III) dimer, dichloro-(pentamethylcyclopentadienyl)iridium(III) dimer, dichloro(tetramethylphenylcyclopentadienyl)iridium(III) dimer, dichloro (tetramethylphenylcyclopentadienyl)-rhodium(III) dimer, dichloro (tetramethyl-biphenylcyclopentadienyl)iridium(III) dimer and dichloro (tetramethylbiphenylcyclopentadienyl l)rhodium (III) dimer were synthesised using a reported microwave method [83].

2.2. Instrumentation

NMR data were acquired on either Bruker DRX-400, Bruker DRX-500 or Varian-300 spectrometers at ambient temperature unless otherwise stated. ^{1}H-NMR chemical shifts were internally referenced to residual protiated MeOD-d_4 (3.49 ppm), acetone-d_6 (2.05 ppm) or $CDCl_3$ (7.26 ppm). High resolution mass spectral data were obtained using methanolic solutions (50% MeOH in H_2O) on a Bruker Esquire 2000 instrument with electrospray as the ionization method. Where stated, microwave syntheses were carried out in a CEM Discover SP microwave reactor. Flash purification of compounds was carried out using a Biotage Isolera One instrument, fitted with a UV–vis detector and running the Spektra package. Purity measurements by HPLC were obtained using the Agilent 1200 system with a VDW and 100 µL loop. The column used was an Agilent Zorbax Eclipse Plus C18, 250 × 4.6 mm with a 5 µm pore size. The mobile phase was H_2O 0.1% TFA/MeOH 0.1% TFA at gradients of $t = 0$ min 10% B, $t = 30$ min 80% B, $t = 40$ min 80% B, $t = 41$ min 10% B, and $t = 55$ min 10% B over a 55 min period. The flow rate was 1 mL min^{-1}, and the detection wavelength was set at 254 nm with the reference wavelength at either 360 or 510 nm. Sample injections were half the loop volume (50 µL) with needle washes of MeOH and H_2O between injections. It was assumed that all species in a sample have the same extinction coefficient at 254 nm. All peaks were manually integrated to gain the percentage areas. Samples were dissolved in 10% CH_3OH/90% H_2O at ca. 100 µM.

2.3. Synthesis of compounds

2.3.1. 4-Methyl-4′-carboxy-2,2′-bipyridine dihydroartemisinin ester (L1)

4-Methyl-4′-carboxy-2,2′-bipyridine (0.428 g, 2.0 mmol) was suspended in anhydrous diethyl ether (30 mL) and cooled to 0 °C. Oxalyl chloride (2 M in DCM, 1.1 mL, 2.20 mmol) was slowly added over 5 min followed by a catalytic amount of anhydrous DMF (50.0 µL). The reaction suspension was stirred under nitrogen gas and allowed to warm to room temperature over 16 h. The solvent was then evaporated under reduced pressure with protection from moisture. The crude acid chloride was dissolved in anhydrous DCM (40.0 mL), cooled to 0 °C and dihydroartemisinin (0.596 g, 2.1 mmol) and triethylamine (607 µL, 6.00 mmol) were added. The reaction was allowed to warm slowly to room temperature with stirring over 6 h. Saturated sodium bicarbonate solution (20.0 mL) was then added, and the mixture was stirred vigorously for 10 min. It was then transferred to a separation funnel and the organic phase collected. The organic phase was washed with sodium bicarbonate, water and brine, dried over sodium sulfate and filtered. Evaporation of the solvent yielded a crude brown residue that was subjected to flash purification to yield the product (**L1**) as a white solid (0.424 g, 44%). Flash chromatography was carried out using ethyl acetate and hexane as elution solvents on a Biotage® SNAP KP-Sil 50 g column. Briefly, the following conditions were used: equilibrate column (3 column volumes (CVs)) with 0% of ethyl acetate and then elution of product with a gradient of 0% ethyl acetate to 100% ethyl acetate over 20 CVs. ^{1}H NMR (400 MHz, chloroform-d_1): δ (ppm) = 8.90 (s, 1H, bipy-

H), 8.75 (d, *J*(H-H): 4.5 Hz, 1H, bipy-H), 8.51 (d, *J*(H-H): 4.5 Hz, 1H, bipy-H), 8.15 (s, 1H, bipy-H), 7.86 (d, *J*(H-H): 5.0 Hz, 1H, bipy-H), 7.09 (d, *J*(H-H): 5.0 Hz, 1H, bipy-H), 5.97 (d, *J*(H-H): 10.0 Hz, 1H, ART-H), 5.45 (s, 1H, ART-H), 2.71–2.77 (m, 1H, ART-H), 2.38 (s, 3H, bipy-CH_3), 2.30–2.33 (m, 1H, ART-H), 1.63–1.85 (m, 7H, ART-H), 1.37 (s, 3H, ART-CH_3), 1.20–1.26 (m, 3H, ART-CH_3), 0.90 (t, *J*(H-H): 8.0 Hz, 6H, ART-CH_3). $^{13}C\{^1H\}$ NMR (101 MHz, acetone-d_6): δ (ppm) = 170.9 ($C{=}O_{ester}$), 164.6 (ART) 158.4, 155.7 (bipy), 151.2, 150.2 (bipy), 138.9 (ART), 1126.20, 123.6, 122.4, 120.7 (bipy), 104.8 (ART), 96.4, 94.4, 92.3, 91.6, 88.2, 80.9, 66.1, 60.6, 52.6, 46.2, 37.7, 37.2, 35.0 32.9, 26.0 (ART), 26.0, 21.2, 20.6, 12.52 (ART-CH_3, bipy-CH_3). HR-ESI-MS for $C_{27}H_{32}N_2O_6$, calculated for ($[M + Na]^+$): 503.2153, found: *m/z* 503.2150 (100%). HPLC purity: 95%; $t_{r'}$ = 12.81 min.

2.3.2. General synthetic method for Rh(III) and Ir(III) bipyridyl-artemisinyl complexes (*1*–*6*)

The ligand, 4-methyl-4′-carboxy-2,2′-bipyridine dihydroartemisinin ester (**L1**, 2 mol equiv) was dissolved in methanol (15 mL) and a solution of the appropriate rhodium or iridium dimer (1 mol equiv.) in DCM (10 mL) was added and the reaction solution was stirred for 16 h at room temperature. Ammonium hexafluorophosphate (2 mol equiv.) was then added and reaction stirred for a further 1 h. The solvent was then evaporated, and the orange yellow residue was re-dissolved in acetone (10 mL) filtered through celite to remove insoluble inorganic salts. The volume of the filtrate was reduced to ca. 3 mL. The product was then precipitated from solution by addition of diethyl ether and isolated by vacuum filtration, washed with diethyl ether and dried.

2.3.2.1. [(η^5-Pentamethylcyclopentadienyl)IrCl(N,N′-methylbipyridylartemisinyl ester)]PF_6 (*1*).

Methyl-4′-carboxy-2,2′-bipyridine dihydroartemisinin ester (**L1**) (0.050 g, 0.104 mmol) was reacted with dichloro(pentamethylcyclopentadienyl)iridium(III) dimer (0.041 g, 0.052 mmol) and ammonium hexafluorophosphate (0.017 g, 0.104 mmol). The product (**1**) was isolated as a bright yellow microcrystalline solid (0.088 g, 86%). ^1H NMR (400 MHz, acetone-d_6): δ (ppm) = 9.33 (d, *J*(H-H): 6.0 Hz, 1H, bipy-H), 9.10 (d, *J*(H-H): 17.1 Hz, 1H, bipy-H), 8.99 (d, *J*(H-H): 6.0 Hz, 1H, bipy-H), 8.86 (s, 1H, bipy-H), 8.38 (t, *J*(H-H): 5.5 Hz, 1H, bipy-H), 7.80 (d, *J*(H-H): 5.5 Hz, 1H, bipy-H), 6.05 (m, 1H, ART-H), 5.69 (s, 1H, ART-H), 2.75–2.65 (m, 3H, ART-CH_3), 2.05 (s, 3H, bipy-CH_3), 1.60–1.95 (m, 22H, ART-H, Cp*-CH_3), 1.45–1.55 (m, 2H, ART-H), 1.11 (s, 3H, ART-CH_3), 0.99 (m, 6H, ART-CH_3). $^{13}C\{^1H\}$ NMR (101 MHz, acetone-d_6): δ (ppm) = 182.2, 179.3, 154.2, 152.2, 145.2, 141.2, 131.0, 130.9, 128.8, 123.7, 118.2, 117.22, 116.7, 104.9, 95.4, 93.8, 92.4, 90.8, 77.6, 52.6, 46.1, 37.7, 37.0, 26.0, 25.4, 22.4, 21.2, 20.5, 14.9, 8.6. HR-ESI-MS for $C_{37}H_{47}ClF_6IrN_2O_6P$, calculated for ($[M - PF_6^-]^+$): 843.2740, found: *m/z* 843.2757 (100%). HPLC purity: >99%; $t_{r'}$ = 9.16 min.

2.3.2.2. [(η^5-Tetramethylphenylcyclopentadienyl)IrCl(N,N′-methylbipyridylartemisinyl ester)]PF_6 (*2*).

Methyl-4′-carboxy-2,2′-bipyridine dihydroartemisinin ester (**L1**) (0.050 g, 0.104 mmol) was reacted with dichloro(tetramethylphenylcyclopentadienyl)iridium(III) dimer (0.048 g, 0.052 mmol) and ammonium hexafluorophosphate (0.017 g, 0.104 mmol). The product (**2**) was isolated as a bright yellow microcrystalline solid (0.104 g, 95%). ^1H NMR (500 MHz, acetone-d_6) δ (ppm) = 9.16 (dd, *J*(H-H) = 4.3, 1.9 Hz, 1H, bipy-H), 9.11 (t, *J* = 5.6 Hz, 1H, bipy-H) 9.00–8.89 (m, 1H, bipy-H), 8.84–8.79 (m, 1H, bipy-H), 8.78–8.67 (m, 1H, bipy-H), 8.34 (m, 1H, bipy-H), 7.77–7.72 (m, 1H, Cp^x-Ar-H), 7.71–7.62 (m, 2H, Cp^x-Ar-H), 7.62–7.50 (m, 2H, Cp^x-Ar-H), 6.12–6.01 (m, 1H, ART-H), 5.68 (d, *J* = 9.6 Hz, 1H, ART-H), 2.75–2.62 (m, 2H, ART-H), 2.34 (m, 1H, ART-H), 2.05 (s, 3H, ART-bipy-CH_3), 2.00–1.88 (m, 8H, ART-H), 1.90–1.40 (m, 16H, ART-H, Cp^x-CH_3), 1.30 (s, 3H, Cp^x-CH_3), 0.98 (s, 3H, Cp^x-CH_3). $^{13}C\{^1H\}$ NMR (126 MHz, acetone-d_6) δ (ppm) = 152.29, 151.38, 150.77, 130.41, 130.11, 129.62, 129.46, 129.21, 125.99, 125.35, 123.92, 123.37, 119.01, 89.84, 44.61, 36.54, 35.80, 31.48, 29.20, 28.90, 24.94, 19.73. HR-ESI-MS for $C_{42}H_{49}ClF_6IrN_2O_6P$, calculated for ($[M - PF_6^-]^+$): 905.2897, found: *m/z* 905.2911 (100%). HPLC purity: >99%; $t_{r'}$ = 14.47 min.

2.3.2.3. [(η^5-(Tetramethylbiphenylcyclopentadienyl)IrCl(N,N′-methylbipyridylarte-misinyl ester)]PF_6 (*3*).

Methyl-4′-carboxy-2,2′-bipyridine dihydroartemisinin ester (**L1**) (0.050 g, 0.104 mmol) was reacted with dichloro(tetramethylbiphenylcyclopentadienyl)iridium(III) dimer (0.056 g, 0.052 mmol) and ammonium hexafluorophosphate (0.017 g, 0.104 mmol). The product (**3**) was isolated as a bright orange microcrystalline solid (0.109 g, 93%). ^1H NMR (500 MHz, acetone-d_6) δ (ppm) = 9.19–9.10 (m, 1H, bipy-H), 9.01–8.92 (m, 1H, bipy-H), 8.90–8.80 (m, 2H, bipy-H), 8.83–8.71 (m, 1H, bipy-H), 8.35 (m, 1H, bipy-H), 7.92–7.72 (m, 7H, Cp^x-Ar-H), 7.58–7.41 (m, 2H, Cp^x-Ar-H), 6.04 (d, *J* = 9.8 Hz, 1H, ART-H), 5.62 (s, 1H, ART-H), 2.75–2.61 (m, 4H, ART-CH_3), 2.39–2.27 (m, 1H, ART-H), 2.16–2.02 (m, 2H, ART-H), 2.00–1.23 (m, 22H, ART-H, Cp^x-CH_3), 1.15–0.96 (m, 6H, ART-H, Cp^x-CH_3). $^{13}C\{^1H\}$ NMR (126 MHz, acetone-d_6) δ (ppm) = 196.55, 194.47, 152.09, 151.28, 131.05, 130.18, 129.64, 129.19, 127.77, 126.88, 125.84, 125.39, 123.43, 89.99,

49.97, 35.01, 31.29, 28.90, 16.50. HR-ESI-MS for $C_{48}H_{53}ClF_6IrN_2O_6P$, calculated for ($[M - PF_6^-]^+$): 981.3211, found: *m/z* 981.3227 (100%). HPLC purity: >99%; $t_{r'}$ = 19.92 (aqua), 21.70 (chloride) min.

2.3.2.4. [(η^5-Pentamethylcyclopentadienyl)RhCl(N,N′-methylbipyridylartemisinyl ester)]PF_6 (*4*).

Methyl-4′-carboxy-2,2′-bipyridine dihydroartemisinin ester (**L1**) (0.050 g, 0.104 mmol) was reacted with dichloro(pentamethylcyclopentadienyl)rhodium(III) dimer (0.032 g, 0.052 mmol) and ammonium hexafluorophosphate (0.017 g, 0.104 mmol). The product (**4**) was isolated as an orange microcrystalline solid (0.083 g, 89%). ^1H NMR (500 MHz, acetone-d_6) δ (ppm) = 9.09–8.90 (m, 1H, bipy-H), 8.82–8.74 (m, 2H, bipy-H), 8.46–8.43 (m, 1H, bipy-H), 8.31–8.30 (m, 1H, bipy-H), 7.69–7.68 (m, 1H, bipy-H), 6.02 (d, *J* = 9.03 Hz, 1H, ART-H), 5.66 (s, 1H, ART-H), 3.42–1.70 (d, *J* = 2.1 Hz, 25H, ART-H, Cp*-CH_3), 1.67–1.45 (m, 3H, ART-H), 1.40–1.26 (m, 4H, ART-H), 1.17–0.88 (m, 7H, ART-H). $^{13}C\{^1H\}$ NMR (126 MHz, acetone-d_6) δ (ppm) = 152.82, 151.74, 136.06, 129.72, 129.45, 128.90, 125.55, 125.11, 123.15, 120.32, 91.59, 90.45, 86.46, 51.74, 34.98, 31.27, 29.21, 28.56, 8.55. HR-ESI-MS for $C_{37}H_{47}ClF_6N_2O_6PRh$, calculated for ($[M - PF_6^-]^+$): 753.2172, found: *m/z* 753.2186 (100%). HPLC purity: >99%; $t_{r'}$ = 10.46 (aqua), 13.31 (chloride) min.

2.3.2.5. [(η^5-Tetramethylphenylcyclopentadienyl)RhCl(N,N′-methylbipyridylartemisinyl ester)]PF_6 (*5*).

Methyl-4′-carboxy-2,2′-bipyridine dihydroartemisinin ester (**L1**) (0.050 g, 0.104 mmol) was reacted with dichloro(tetramethylphenylcyclopentadienyl)rhodium(III) dimer (0.039 g, 0.052 mmol) and ammonium hexafluorophosphate (0.017 g, 0.104 mmol). The product (**5**) was isolated as an orange microcrystalline solid (0.088 g, 88%). ^1H NMR (500 MHz, acetone-d_6) δ 9.09–8.98 (m, 2H, bipy-H), 8.82 (m, 1H, bipy-H), 8.72–8.63 (m, 1H, bipy-H), 8.35 (m, 1H, bipy-H), 7.83–7.55 (m, 6H, Cp^x-Ar-H, bipy-H), 6.04 (dd, *J* = 9.8, 3.9 Hz, 1H), 5.68 (d, *J* = 13.3 Hz, 1H), 2.74–2.61 (m, 4H), 2.39–2.27 (m, 1H), 2.12–2.06 (m, 4H), 1.99–1.90 (m, 8H), 1.91–1.74 (m, 8H), 1.78–0.94 (m, 11H, ART-H, Cp^x-CH_3). $^{13}C\{^1H\}$ NMR (126 MHz, acetone-d_6) δ (ppm) = 152.42, 151.22, 130.90, 130.58, 129.77, 129.69, 129.63, 129.44, 128.48, 125.99, 125.18, 123.49, 91.34, 44.89, 43.92, 36.47, 35.63, 31.44, 24.81, 9.95. HR-ESI-MS for $C_{42}H_{49}ClF_6N_2O_6PRh$, calculated for ($[M - PF_6^-]^+$): 815.2329, found: *m/z* 815.2343 (100%). HPLC purity: 96%; $t_{r'}$ = 12.80 (aqua), 16.99 (chloride) min.

*2.3.2.6. [η^5-(Tetramethylbiphenylcyclopentadienyl)RhCl(N,N′-methyl-bipyridylartemisinyl ester)]PF_6 (**6**).* Methyl-4′-carboxy-2,2′-bipyridine dihydroartemisinin ester (**L1**) (0.050 g, 0.104 mmol) was reacted with dichloro(tetramethylbiphenylcyclopentadienyl)rhodium(III) dimer (0.046 g, 0.052 mmol) and ammonium hexafluorophosphate (0.017 g, 0.104 mmol). The product (**6**) was isolated as a bright orange microcrystalline solid (0.100 g, 93%). ^{1}H NMR (500 MHz, acetone-d_6) δ 9.09–8.98 (m, 2H, bipy-H), 8.83–8.70 (m, 2H, bipy-H), 8.37–8.33 (m, 1H, bipy-H), 7.93–7.89 (m, 4H, Cp^x-Ar-H, bipy-H), 7.83–7.72 (m, 3H, Cp^x-Ar-H), 7.56–7.40 (m, 3H, Cp^x-Ar-H), 6.01 (d, $J = 9.6$ Hz, 1H, ART-H), 5.64 (d, $J = 24.3$ Hz, 1H, ART-H), 2.70–2.54 (m, 4H, ART-H, ART-CH_3), 2.31 (t, $J = 13.7$ Hz, 1H, ART-H), 2.09–1.35 (m, 25H, ART-H, Cp^x-CH_3), 0.97–0.90 (m, 6H, ART-H, Cp^x-CH_3). ^{13}C{^{1}H} NMR (126 MHz, acetone-d_6) δ (ppm) = 161.83, 155.92, 153.35, 153.09, 152.95, 152.53, 151.04, 141.86, 140.42, 139.58, 135.13, 131.12, 129.66, 129.46, 129.12, 128.97, 128.10, 127.90, 127.66, 127.54, 127.38, 127.09, 126.88, 126.83, 126.78, 125.44, 125.21, 122.84, 122.70, 105.53, 104.02, 95.78, 95.68, 95.64, 91.50, 90.97, 89.47, 80.00, 51.58, 45.18, 44.40, 37.02, 36.74, 36.67, 36.05, 34.22, 34.00, 31.88, 31.76, 29.69, 29.62, 25.14, 24.50, 24.32, 21.51, 20.29, 19.62, 11.53, 9.62, 8.01. HR-ESI-MS for $C_{48}H_{53}ClF_6N_2O_6PRh$, calculated for ($[M-PF_6^-]^+$): 891.2642, found: *m/z* 891.2641 (100%). HPLC purity: 97%; t_r = 19.35 min.

2.4. Biological activity

2.4.1. Evaluation of in vitro activity against P. falciparum asexual blood stages

Compounds were solubilized in 100% DMSO to a final concentration of 5 mM. The stock solutions of compounds were then diluted further in DMSO to generate dose response dilutions (3 doses per log) in 384-well polypropylene compound storage plates. The dose response dilution plates were generated by dilution of 1 μL into 25 μL of sterile water and 5 μL transferred into 384-well imaging plates. The confocal image analysis assay is published in detail elsewhere [84]. In brief, *P. falciparum* 3D7 and Dd2 strains were kept in continuous culture (Roswell Park Memorial Institute medium (RPMI) supplemented with, 25 mM Hepes, 50 μg/mL hypoxanthine, 2.5 mg/mL Albumax II® plus 5% human serum) with sorbitol synchronization performed over two successive intra erythrocytic lifecycles to provide ring-stage parasites for use within the assays. On the day of assay, ring-stage parasite culture was adjusted to 2% parasitemia and 0.3% hematocrit and 45 μL of which was added to the compound-containing imaging plates. The assay plates were incubated for 72 h at 5% O_2, 5% CO_2 and 90% N_2. The plates were removed from incubation and allowed to equilibrate at room temperature prior to staining with 4′,6-diamidino-2-phenylindole (DAPI). The imaging assay plates were then imaged on an Opera confocal imaging system (Perkin Elmer). Using Accapella scripting software, the number of classified parasites was determined for each assay well. Percent inhibition of parasite proliferation was calculated and normalized to assay control data of 0.4% DMSO and 5 μM Puromycin. Percent inhibition of parasite numbers (normalized to 5 μM puromycin) was plotted against log concentration of the compounds using a 4-parameter log dose, non-linear regression analysis, with sigmoidal dose response (variable slope) curve fit using Prizm 4.0. No constraints were placed on the top, bottom or Hill slope of the curve fit in the graphing software. The resistance index (RI) was determined using the equation:

$$RI = \frac{IC_{50}(Dd2)}{IC_{50}(3D7)}$$

RI < 1 indicates compounds are more active in the drug resistant *Pf* strain (Dd2)

RI ≈ 1 indicates that compounds show similar activities in both the drug sensitive and drug resistant *Pf* strains

RI > 1 indicates that compounds are more active in the drug sensitive *Pf* strain (3D7)

2.4.2. Evaluation of plasmodial gametocytocidal in vitro activity

The assay is described elsewhere in detail [85,86]. In brief, the assay uses highly synchronous stage IV gametocytes induced from a transgenic NF54-$^{pfs16\text{-}Luc\text{-}GFP}$ parasite strain [87]. The gametocytes were harvested by magnetic isolation on day 9 and then added (45 μL of 10% gametocytes at 0.1% haematocrit) to the test compounds in 384 well imaging plates as described for the asexual blood stage *P. falciparum* assay above. Following the addition of the parasite to the test compounds, the plates were incubated for 72 h under reduced oxygen tension (5% CO_2, 5% O_2, 80% N_2). After incubation, Mitotracker Red CMH2XRos was added to the plates, which were then incubated overnight in standard conditions. After overnight incubation, the plates were imaged on the Opera confocal imaging system. Images for green fluorescent protein (GFP) and Mitotracker Red were overlaid and the number of elongated viable gametocytes per image determined using a script based on Acapella software developed for use with the Opera imaging system. The average Mitotracker Red fluorescence intensity was determined for objects greater than a determined size. Objects which were more than three times longer than they are wide were identified using the GFP images and are representative of gametocytes. Objects which were elongated and had Mitotracker Red fluorescent intensity above the cut-off limit were then identified as viable gametocytes. Using DMSO and 5 μM puromycin as controls, the relative percent inhibition was calculated for the compounds. IC_{50} values were then calculated as described for the *P. falciparum* asexual blood stage assay described above.

2.4.3. Human embryonic kidney (HEK293) mammalian cell cytotoxicity [88]

HEK293 cells were cultured in Dulbecco's Modified Eagle Medium (DMEM) supplemented with 10% Fetal Bovine Serum (FBS). The cells were harvested and dispensed into 384 well sterile black, clear base microtiter plates at 2000 cells/well (45 μL). The plates were left to settle, and the cells attach overnight in a standard tissue culture incubator at 5% CO_2, 37 °C and 60% humidity. After overnight incubation, 5 μL of diluted compound (as described in the section, Evaluation of *in vitro* activity against *P. falciparum* asexual blood stages) was added to the cell containing plates and incubated for a further 72 h. After incubation, the supernatant from the wells was removed and 40 μl of 40 μM resazurin in DMEM media (FBS free) added to all wells. The plates were incubated for 6 h then measured for fluorescent intensity using the PerkinElmer Envision. The data were analysed as in the *Plasmodium falciparum* methods section.

2.4.4. Trichomonal growth inhibition assays

Cultures of *T. vaginalis* strain G3 were grown and maintained in 11 mL of TYM (trypticase, yeast extract and maltose) Diamond medium at pH 6.2. Parasite inhibitory screens were carried out as previously described [51]. These assays were incubated at 37 °C for 24 h before being counted using a hemocytometer. Percentage inhibitory activities were calculated relative to the DMSO control. Stock solutions were diluted in media and tested over a range of increasing concentrations. All screening trials were performed a minimum of three times on three separate days to a standard error of ≤0.10.

2.4.5. Disc diffusion antibiotic sensitivity assay on pathogenic and normal flora bacteria

Pathogens such as *Salmonella enterica* pGFP and *Listeria monocytogenes* 10403 (RM2194) or non-pathogens and commensals *Escherichia coli* K-12 MG 1655, *Lactobacillus reuteri* (ATCC 23272), *Lactobacillus acidophilus* (ATCC 43560), and *Lactobacillus rhamnosus* (ATCC 53103) were grown in Luria Broth (LB), Brain Heart Infusion Broth (BHI), or *Lactobacilli* MRS at 37 °C overnight aerobically, but *Lactobacilli* strains were grown under anaerobic conditions. Saturated overnight cultures were streaked onto respective media agar plates with sterile wood cotton sticks to form a continuous lawn of bacterial growth. 100 mM stock solutions in DMSO were diluted into media to a final concentration of

100 μM as well as a vehicle control. 6 mm blank BDL-sensi-discs were incubated with the 100 μM compounds or vehicle control at room temperature for 20 min. BDL-antibiotic laden discs containing levofloxacin (5 μg), gentamicin (10 μg), and gentamicin (120 μg) were used as controls for antibiotic sensitivity. Discs were subsequently placed onto the bacterial streaked agar plates and incubated overnight at 37 °C. Zones of inhibition representing antibiotic and/or compound sensitivity were measured in mm for each of the antibiotics, compounds, and vehicle controls.

3. Results and discussion

3.1. Synthesis and characterization

Reduction of the carbonyl of the lactone in artemisinin (**ART**) using sodium borohydride yielded the intermediate, dihydroartemisinin (**DHA**) which was isolated as a near 1:1 mixture of α- and β- epimers (Scheme 1) [89]. These epimers were identified from the NMR coupling constants of the proton on C-7 (Supplementary Fig. S1). **DHA** was then reacted with 4′-methyl-[2,2′-bipyridine]-4-carbonyl chloride, produced *in situ* by reaction of 4′-methyl-[2,2′-bipyridine]-4-carboxylic acid with oxalyl chloride, with Et_3N as base to give the ligand **L1** in moderate yields (Scheme 1). Haynes *et al* have previously reported that reaction of **DHA** with acid chlorides in the presence of Et_3N favoured formation of α-ester products [89]. Using their data as a guide, we identified by ^1H NMR that the α-epimer of **L1** was the major product isolated (Supplementary Fig. S1). For **L1**, a coupling constant of 10.0 Hz was observed for the proton of C-7. In the α-conformation, this proton and the proton of C-8 are in a *trans*-diaxial position relative to each other leading to a larger coupling contant. The protons of the bipyridyl rings were observed between 8.90 and 7.09 ppm with the expected multiplicity for each proton. The methyl group of the 4′-methyl-2,2′-bipyridyl group resonates as a singlet at 2.38 ppm. Isolation of **L1** was also confirmed with HR-ESI-MS where the base peak is the sodium adduct ($[M + Na]^+$) of **L1**.

The cationic complexes **1–6** were synthesised by dropwise addition of a DCM solution of the appropriate iridium or rhodium dimer to a methanolic solution of **L1** at room temperature followed by addition of ammonium hexafluorophosphate. Chelation of **L1** to the metal via the nitrogen atoms was confirmed by the downfield shift of the protons adjacent to the nitrogen for each pyridyl ring. The protons resonate at 8.75 and 8.51 ppm in the free ligand, and are observed between 9.35 and 9.00 ppm for the complexes. For the complexes containing the Cp^x ligand, **2** and **5** (Cp^{xph}) and **3** and **6** (Cp^{xbiph}), the aromatic protons for this ligand resonate at lower frequencies compared to the bipyridyl group. The methyl protons for the Cp ring for all complexes overlap with the alkyl protons of the artemisinyl group. HPLC analysis confirmed the high purity (96–99%) of the products isolated (Supplementary Figs. S2–S8) and complexes **1–6** displayed a base peak for the $[M\text{-}PF_6]^+$ molecular ion in the HR-ESI-MS (Supplementary Figs. S9–S15).

3.2. Antiparasitic activity

The *in vitro* inhibitory activities of **L1** and complexes **1–6** were determined on two *Pf* strains (asexual) and late stage gametocytes, plus a *Trichomonas vaginalis* (*Tv*) strain.

To evaluate antiplasmodial activity, the complexes were screened against 3D7 (sensitive), Dd2 (multi drug resistant) strains plus NF54 late stage gametocytes (LSGNF54). Except for complex **5**, the complexes and the free ligand exhibit activity in the nanomolar range and are significantly more active *in vitro* than chloroquine against all parasite cultures (Table 1). The assays were carried out in duplicate for three independent biological replicates. **L1** was more active than the complexes **1–6**. Incorporation of the Ir(III) and Rh(III) Cp^x fragments appears to lead to a decrease in activity. Nevertheless, compared to artemisinin, complexes **1–4** and **6** are still potent *Pf* inhibitors and should be explored further against other *Pf* strains. The data from this *in vitro* assay show **L1** is only ≈ 3 times more active than the complex showing the best antiplasmodial activity (complex **1**). Further *in vitro* as well as *in vivo* testing of these complexes could reveal that the complexes have similar or better activity than **L1**. Thus, further studies are essential before it can be said that Rh(III) and Ir(III) complexes containing ART derivatives should not be developed further. Additionally, incorporation of the substituted cyclopentadienyl Ir(III) and Rh(III) moieties may modify the mode of action of drug candidates. For example, Ir(III) and Rh(III) complexes can act as intracellular transfer hydrogenation catalysts for the conversion of β-nicotinamide adenine dinucleotide (NAD^+) to reduced β-nicotinamide adenine dinucleotide (NADH) [90], a trait that has been applied in the development of these compounds as anticancer agents. Recently, it was also reported that Cp*Ir(III) complexes are able to catalytically affect the NAD^+/NADH ratio in a modified *Plasmodium* lactate dehydrogenase (pLDH) assay when dosed with the hydride source sodium formate [91,92] and a significant decrease in parasite viability was observed in the CQ-resistant K1 strain when one of these complexes was assayed with varying concentrations of sodium formate [91]. Therefore, while addition of the Cp^x Ir(III) and Rh(III) moieties to **L1** leads to a slight decrease in activity, this could be countered by the addition of an alternative mode of action that may not be readily blocked by the parasite.

There are only a few previous reports of *in vitro* antimalarial activity of organo-Rh(III) and -Ir(III) half-sandwich complexes. Ekengard et al. found good to moderate activity for their Cp* complexes containing NˆN and NˆO-chelated chloroquine analogues towards chloroquine sensitive (CQS) NF54 and the chloroquine resistant (CQR) Dd2 strains of *Plasmodium falciparum* [93]. They also reported that Rh(III) and Ir(III) Cp* complexes containing aminoquinoline hybrids with pharmacophores from tuberculosis drugs, had moderate anti-plasmodial and anti-mycobacterial activity, the complexes being over an order of magnitude more active than the free ligands [94]. Also, we reported that cyclopentadienyl Rh(III) and Ir(III) complexes containing an N,N′-

Table 1
Summary of IC_{50} data for ligand **L1**, complexes **1–6**, and the control drugs, chloroquine (**CQ**), artesunate (**ARS**), dihydroartemisinin (**DHA**) and artemisinin (**ART**) in *Pf* strains 3D7 (sensitive), Dd2 (multidrug resistant) and late stage gametocyte (LSG) NF54 (sexual) and the human embryonic kidney cell line HEK293. $N = 3$ biological replicates in duplicate point.

	Pf 3D7	*Pf* Dd2	Resistance index	*Pf* LSG	HEK293
Compound	IC_{50} (nM)[a]	IC_{50} (nM)[a]	Dd2/3D7	IC_{50} (nM)[a]	IC_{50}[a]
L1	0.14 (0.01)	0.17 (0.06)	1.3	7.36 (4.30)	IA[b]
1	0.42 (0.17)	0.53 (0.14)	1.3	20.1 (10.9)	IA
2	0.55 (0.14)	0.83 (0.28)	1.5	8.38 (0.55)	IA
3	0.61 (0.42)	1.19 (0.35)	1.9	25.8 (15.2)	IA
4	1.16 (0.41)	1.99 (0.37)	1.7	47.3 (17.3)	IA
5	63.9 (14.8)	81.7 (18.9)	1.3	764.0 (103.2)	IA
6	1.27 (0.19)	1.80 (0.31)	1.4	70.9 (36.4)	IA
CQ	11.8 (1.2)	60.0 (9.3)	5.1	$> 20 \times 10^3$	IA
ARS	0.90 (0.05)	1.07 (0.02)	1.2	6.99 (0.49)	IA
DHA	0.73 (0.04)	0.72 (0.11)	1.0	11.2 (6.4)	IA
ART	2.18 (0.41)	2.91 (0.38)	1.3	8.37 (2.31)	IA

[a] Standard deviation given in parentheses.
[b] IA: inactive at 20 μM.

chelated pyridylimino-or quinolylimino ligands functionalized with the antimalarial drug sulfadoxine exhibit potent (0.10–2.0 μM) antiplasmodial activity in *P. falciparum* assays (3D7 chloroquine sensitive, Dd2 chloroquine resistant and NF54 sexual late stage gametocytes), but were only moderately active towards *Trichomonas vaginalis* [95].

Complexes **1–4** and **6** are 2–4 times more active than artemisinin against the 3D7 and Dd2 parasite strains. The iridium complexes (**1–3**) appear to be 2–4 times more active than the rhodium derivatives (**4–6**). The data for the iridium complexes on the asexual intra-erythrocytic parasites (3D7 and Dd2) revealed that the Cp*Ir complex **1** has similar or higher activity than the Cp^{xph} (**2**) and Cp^{xbiph} (**3**) Ir complexes (IC_{50}: **1** = 0.42 nM (3D7), 0.17 nM (Dd2); **2** = 0.55 nM (3D7), 0.83 nM (Dd2); **3** = 0.61 nM (3D7), 1.99 nM (Dd2)). In the drug resistant Dd2 strain there is a clear decrease in activity as the cyclopentadienyl ring is extended from Cp* to Cp^{xph} and Cp^{xbiph} for the iridium complexes. It is possible that the increasing hydrophobic character of these compounds affects their activity, or that these compounds act via a different mode of action on the drug resistant Dd2 strain compared to the drug sensitive 3D7 strain.

However, when the complexes were tested on late stage gametocytes (LSG NF54), complex **2** (Cp^{*ph}) showed the highest activity (IC_{50} = 8.38 nM), which is comparable to the IC_{50} value for **L1** (IC_{50} = 7.36 nM) and ART (IC_{50} = 8.37 nM). The iridium complexes showed better activities than DHA (IC_{50} = 0.73 nM (3D7), 0.72 nM (Dd2)). The rhodium complexes **4** and **6** had similar IC_{50} values for the 3D7 and Dd2 strains while complex **5** showed a much lower activity towards these two strains. It is not clear why complex **5** has such low activity compared to the Rh(III) analogues **4** and **6** or its Ir(III) derivative complex **2** since they are structurally similar.

Comparison of the activity of **1–6** between 3D7 and Dd2, demonstrates no selectivity for the complexes between the CQ-sensitive 3D7 and the CQ-resistant Dd2 strains based on the resistance index. None of the compounds were cytotoxic against the HEK293 cell line at concentrations up to 20 μM.

Trichomoniasis is caused by *Trichomonas vaginalis* (*T. vaginalis*), a sexually transmitted protozoan parasite, that infects the urogenital tract of humans. Screening of the complexes against the *T. vaginalis* strain G3 showed low-to-no activity towards this parasite (Table 2). Complexes **3–6** were the only complexes with any significant percent inhibition, but their IC_{50} values were moderate (24–34 μM). These compounds also showed no detectable effects on a number of different human pathogenic and normal flora bacteria (data not shown).

3.3. Anticancer acivity

The antiproliferative activity of the complexes was determined on five human cancer cell lines, A2780 (ovarian carcinoma), A549 (alveolar adenocarcinoma), HCT116 (colorectal carcinoma), and MCF7 (breast), and PC3 (prostate), Table 3 and Fig. 2.

Similar to the antiplasmodial assays, the iridium complexes (**1–3**) were more active than the rhodium complexes (**4–6**). **ART** shows no appreciable activity across all four cell lines while **DHA** was active only against the A2780 (IC_{50} = 4.73 μM) and PC3 (IC_{50} = 14.1 μM) cell lines. The iridium complexes **1–3** were more potent (IC_{50} = 2.49 (**1**), 0.89 (**2**), 1.06 (**3**) μM) than **DHA** against the A2780 cell line and all of the complexes were better inhibitors of cell growth than **DHA** against the PC3 cell line.

We have shown previously that $[(Cp^*)Ir(bipyridine)Cl]^+$ is inactive towards A2780 ovarian cancer cells, but activity is switched on by replacement of a methyl substitutent on Cp* by a phenyl (Cp^{xph}) or biphenyl (Cp^{xbip}) group [96]. Similarly, the Rh(III) bipyridyl analogue $[(Cp^*)IRh(bipyridine)Cl]^+$ is relatively inactive agaist A2780 cells (IC_{50}: 64 μM), but the activity improves a little (IC_{50}: 36 μM) with a biphenyl substituent on the tetramethylcyclopentadienyl ring [97]. The marked

Table 2
Percent inhibition and IC_{50} values for ligand **L1** and complexes **1–6** against *Tv* strain G3.

Compound	% inhibition at 100 μM[a]	IC_{50} (μM)[b]
L1	18.06 (0.16)	nt[c]
1	5.78 (0.12)	nt[c]
2	51.70 (0.08)	nt[c]
3	95.07 (0.05)	25.91 (0.98)
4	74.05 (0.12)	28.23 (0.99)
5	77.89 (0.10)	33.82 (0.98)
6	97.49 (0.04)	23.92 (0.99)

[a] Standard deviation given in parentheses,
[b] R-squared value given in parentheses,
[c] not tested – IC_{50} not determined as they were considered not to have significant activity based on their % inhibition data.

Table 3
IC_{50} values (μM) for complexes **1–6**, dihydroartemisinin (**DHA**), artemisinin (**ART**) and cis-diamminedichloridoplatinum(II) (**CDDP**) in human cancer cell lines, A2780 (ovarian carcinoma), A549 (alveolar adenocarcinoma), HCT116 (colorectal carcinoma), MCF7 (breast) and PC3 (prostate).

	Cell line				
Compound	A2780[a] (μM)[f]	A549[b] (μM)[f]	HCT116[c] (μM)[f]	MCF7[d] (μM)[f]	PC3[e] (μM)[f]
1	2.49 (0.2)	22.9 (0.7)	19.1 (0.6)	17.5 (0.3)	9.02 (0.44)
2	0.89 (0.09)	10.7 (0.3)	49.5 (0.81)	7.2 (0.8)	5.77 (0.56)
3	1.06 (0.02)	1.82 (0.06)	2.22 (0.18)	1.5 (0.2)	9.23 (0.45)
4	12.7 (0.2)	22.0 (1.0)	24.9 (0.7)	16.5 (0.2)	13.4 (2)
5	6.10 (0.5)	11.56 (0.03)	15.8 (0.3)	11.9 (0.6)	8.91 (0.09)
6	5.38 (0.53)	5.76 (0.37)	8.62 (0.42)	6.5 (0.4)	3.57 (0.58)
ART	>50[g]	>50	>50	>50	>50
DHA	4.73 (0.38)	>50	>50	>50	14.1 (0.5)
CDDP	1.2 (0.2)	4.04 (0.02)	5.76 (0.37)	7.2 (0.5)	0.24 (0.02)

[a] Epithelial, primary tumour, untreated patient,
[b] Epithelial, primary tumour,
[c] Epithelial-like, primary tumour,
[d] Epithelial-like, primary tumour, express both the wild type and variant oestrogen receptors as well as progesterone receptor,
[e] Epithelial, primary tumour,
[f] Results are based on duplicates of triplicates in two biological replicates, Standard deviation given in parenthesis,
[g] not active up to 50 μM.

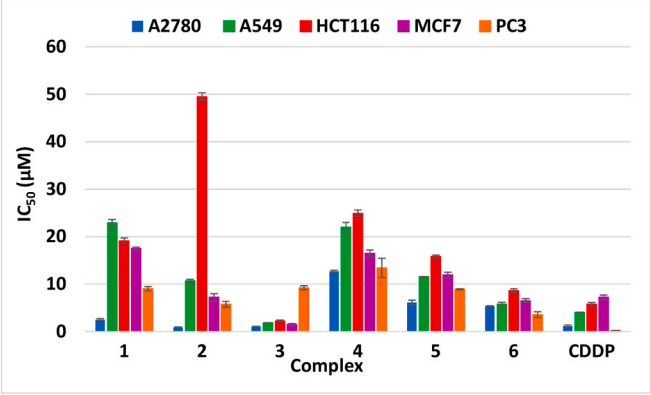

Fig. 2. Graphical representation of the IC_{50} values for complexes **1–6** against the human cancer cell lines A2780 ovarian (blue), A549 lung (green), HCT116 colon (red), MCF7 breast (purple) and PC3 prostate (orange).

increase in potency for the bipyridyl conjugates studied here is therefore apparent (Table 3).

For all cell lines, the complexes with the extended Cp^x group (**2**, **3**, **5** and **6**) are more active than their Cp* counterparts (**1** and **4**). For the A549 lung cancer cell line, complex **3** displays the highest activity, with an IC_{50} that is 2.2× lower than cis-diamminedichloridoplatinum(II) (cisplatin, **CDDP**) while its rhodium analogue, complex **6**, is slightly less active than **CDDP**; the same trend is observed for the HCT116 colon cancer cell line. For the iridium complexes, the Cp* complex **1** is much more active than the Cp^{xph} complex **2** towards HCT116, while the opposite trend is observed for the other cell lines. It is notable that the IC_{50} values for complexes **3** and **6** are mostly in a similar range for all five cell lines (**3**: $IC_{50} = 1.06$ (A2780), 1.82 (A549), 2.22 (HCT116), 1.50 (MCF7), 9.23 (PC3) μM and **6**: $IC_{50} = 5.38$ (A2780), 5.76 (A549), 8.62 (HCT116), 6.50 (MCF7), 3.57 (PC3) μM). These preliminary studies suggest that when compared to **CDDP**, complex **3** has either similar (A2780) or higher (A549, HCT116 and MCF7) activity. In future work it will be interesting to compare the activity, uptake and accumulation of these complexes in cancer cells and normal mammalian cells in comparison with the free ligand **L1**, and to investigate the roles of the organometallic fragments in their mechanism of action. Thus, these complexes show promising anticancer activity, and provide a basis for further development of this class of organometallic complexes in order to optimise activity and selectivity.

4. Conclusions

A new dipyridyl ester derivative of ART (**L1**) was synthesised which formed *N,N′*-coordination complexes with various Ir(III) and Rh(III) half-sandwich fragments to give six cationic complexes **1–6** which differed in the substituents on the cyclopentadienyl ligand (Cp*, Cp^{xph} or Cp^{xbiph}). *In vitro* inhibitory whole cell assays against different parasite strains and cancer cell lines showed that these compounds have high potential as both antiplasmodial and anticancer agents. For the *Pf* strains 3D7 and Dd2, most of these new organometallic complexes displayed activities lower than 2 nM with potencies higher than ART and CQ, and similar to DHA, while they were only moderately active on late stage gametocytes, showing that they may target the asexual stage of the malaria life cycle. The Ir(III) complexes were consistently more active than the Rh(III) analogues towards the *Pf* strains and cancer cell lines, and appear to have no appreciable toxicity towards the healthy cells HEK293. Complex **3** emerged as the most potent compound in this series of new artemisinin-containing organometallic complexes, with anticancer activity comparable to the clinical drug cisplatin.

Declaration of Competing Interest

The authors have no conflicts of interest.

Acknowledgements

We thank the National Research Foundation (NRF) of South Africa (Postdoctoral fellowship 88250), ERC (grant 247450), and EPSRC (grants EP/F034210/1 and EP/P030572/1) for support. KML was supported by the Department of Biological Sciences at the University of the Pacific. This work was supported by the National Health and Medical Research Council (NHMRC) Postgraduate Scholarship (APP1150359); Griffith University Postgraduate Scholarship and Discovery Biology Scholarship awarded to Sandra Duffy. We thank Griffith University and Medicines for Malaria venture for ongoing support. We thank the Australian Red Cross Blood Bank for the provision of fresh red blood cells, without which the *Plasmodium falciparum* research could not have been performed. CCT, JHK, and LWC conducted this research under USDA-ARS CRIS Project 5325-42000-039-00D.

Appendix A. Supplementary data

Supplementary data to this article can be found online at https://doi.org/10.1016/j.jinorgbio.2021.111408.

References

[1] C. Imberti, P. Zhang, H. Huang, P.J. Sadler, Angew. Chem. Int. Ed. 59 (2020) 61–73.
[2] P. Zhang, P.J. Sadler, Eur. J. Inorg. Chem. 2017 (2017) 1541–1548.
[3] D.-L. Ma, C. Wu, G. Li, T.-L. Yung, C.-H. Leung, J. Mater. Chem. B 8 (2020) 4715–4725.
[4] S. Bellemin-Laponnaz, Eur. J. Inorg. Chem. 2020 (2020) 10–20.
[5] P. Chellan, P.J. Sadler, Chem. Eur. J. 26 (2020) 8676–8688.
[6] A. Frei, J. Zuegg, A.G. Elliott, M. Baker, S. Braese, C. Brown, F. Chen, C.G. Dowson, G. Dujardin, N. Jung, A.P. King, A.M. Mansour, M. Massi, J. Moat, H.A. Mohamed, A.K. Renfrew, P.J. Rutledge, P.J. Sadler, M.H. Todd, C.E. Willans, J.J. Wilson, M. A. Cooper, M.A.T. Blaskovich, Chem. Sci. 11 (2020) 2627–2639.
[7] Y.C. Ong, S. Roy, P.C. Andrews, G. Gasser, Chem. Rev. 119 (2019) 730–796.
[8] B. Englinger, C. Pirker, P. Heffeter, A. Terenzi, C.R. Kowol, B.K. Keppler, W. Berger, Chem. Rev. 119 (2019) 1519–1624.
[9] N.P.E. Barry, P.J. Sadler, Chem. Commun. 49 (2013) 5106–5131.
[10] S. Dilruba, G.V. Kalayda, Cancer Chemother. Pharmacol. 77 (2016) 1103–1124.
[11] V. Brabec, J. Kasparkova, Drug Resist. Updat. 8 (2005) 131–146.
[12] R.G. Kenny, C.J. Marmion, Chem. Rev. 119 (2019) 1058–1137.
[13] E. Alessio, G. Mestroni, G. Nardin, W.M. Attia, M. Calligaris, G. Sava, S. Zorzet, Inorg. Chem. 27 (1988) 4099–4106.
[14] G. Mestroni, E. Alessio, G. Sava, S. Pacor, M. Coluccia, A. Boccarelli, Metal-Based Drugs 1 (1994) 41–63.
[15] I. Bratsos, A. Bergamo, G. Sava, T. Gianferrara, E. Zangrando, E. Alessio, J. Inorg. Biochem. 102 (2008) 606–617.
[16] G. Sava, S. Zorzet, C. Turrin, F. Vita, M. Soranzo, G. Zabucchi, M. Cocchietto, A. Bergamo, S. DiGiovine, G. Pezzoni, L. Sartor, S. Garbisa, Clin. Cancer Res. 9 (2003) 1898–1905.
[17] I. Bratsos, S. Jedner, T. Gianferrara, E. Alessio, Chimia 61 (2007) 692–697.
[18] A. Bergamo, G. Sava, Dalton Trans. (2007) 1267–1272.
[19] G. Sava, I. Capozzi, K. Clerici, G. Gagliardi, E. Alessio, G. Mestroni, Clin. Exp. Metastasis 16 (1998) 371–379.
[20] A. Bergamo, C. Gaiddon, J.H.M. Schellens, J.H. Beijnen, G. Sava, J. Inorg. Biochem. 106 (2012) 90–99.
[21] S. Leijen, S.A. Burgers, P. Baas, D. Pluim, M. Tibben, E. van Werkhoven, E. Alessio, G. Sava, J.H. Beijnen, J.H.M. Schellens, Investig. New Drugs 33 (2015) 201–214.
[22] S. Leijen, S.A. Burgers, P. Baas, D. Pluim, M. Tibben, E. van Werkhoven, E. Alessio, G. Sava, J.H. Beijnen, J.H.M. Schellens, Investig. New Drugs 33 (2015) 201–214.
[23] C.G. Hartinger, M.A. Jakupec, S. Zorbas-Seifried, M. Groessl, A. Egger, W. Berger, H. Zorbas, P.J. Dyson, B.K. Keppler, Chem. Biodivers. 5 (2008) 2140–2155.
[24] F. Lentz, A. Drescher, A. Lindauer, M. Henke, R.A. Hilger, C.G. Hartinger, M. E. Scheulen, C. Dittrich, B.K. Keppler, U. Jaehde, Anti-Cancer Drugs 20 (2009) 97–103.
[25] M. Groessl, E. Reisner, C.G. Hartinger, R. Eichinger, O. Semenova, A.R. Timerbaev, M.A. Jakupec, V.B. Arion, B.K. Keppler, J. Med. Chem. 50 (2007) 2185–2193.
[26] S. Kapitza, M. Pongratz, M.A. Jakupec, P. Heffeter, W. Berger, L. Lackinger, B. K. Keppler, B. Marian, J. Cancer Res. Clin. Oncol. 131 (2005) 101–110.
[27] A.V. Vargiu, A. Robertazzi, A. Magistrato, P. Ruggerone, P. Carloni, J. Phys. Chem. B 112 (2008) 4401–4409.
[28] E. Reisner, V.B. Arion, B.K. Keppler, A.J.L. Pombeiro, Inorg. Chim. Acta 361 (2008) 1569–1583.
[29] B.K. Keppler (WO Application 2002059135), Chem. Abstr. 137 (2002), 119658.
[30] R. Trondl, P. Heffeter, C.R. Kowol, M.A. Jakupec, W. Berger, B.K. Keppler, Chem. Sci. 5 (2014) 2925–2932.
[31] S.M. Meier-Menches, C. Gerner, W. Berger, C.G. Hartinger, B.K. Keppler, Chem. Soc. Rev. 47 (2018) 909–928.
[32] P.S. Kuhn, V. Pichler, A. Roller, M. Hejl, M.A. Jakupec, W. Kandioller, B.K. Keppler, Dalton Trans. 44 (2015) 659–668.
[33] S. Silvestri, I. Cirilli, F. Marcheggiani, P. Dludla, G. Lupidi, R. Pettinari, F. Marchetti, C. Di Nicola, G. Falcioni, C. Marchini, P. Orlando, L. Tiano, A. Amici, Mitochondrion 56 (2021) 25–34.
[34] D. Gambino, L. Otero, Inorg. Chim. Acta 393 (2012) 103–114.
[35] R.A. Sanchez-Delgado, A. Anzellotti, Mini-Rev. Med. Chem. 4 (2004) 23–30.
[36] A.L. Noffke, A. Habtemariam, A.M. Pizarro, P.J. Sadler, Chem. Commun. 48 (2012) 5219–5246.
[37] D. Gambino, L. Otero, Inorg. Chim. Acta 472 (2018) 58–75.
[38] S. Monro, K.L. Colón, H. Yin, J. Roque, P. Konda, S. Gujar, R.P. Thummel, L. Lilge, C.G. Cameron, S.A. McFarland, Chem. Rev. 119 (2019) 797–828.
[39] P. Moharana, D. Ghosh, P. Paira, Inorg. Chem. Commun. 124 (2021) 108364.
[40] E.J. Anthony, E.M. Bolitho, H.E. Bridgewater, O.W.L. Carter, J.M. Donnelly, C. Imberti, E.C. Lant, F. Lermyte, R.J. Needham, M. Palau, P.J. Sadler, H. Shi, F.-X. Wang, W.-Y. Zhang, Z. Zhang, Chem. Sci. 11 (2020) 12888–12917.
[41] S. Harringer, M. Matzinger, N. Gajic, M. Hejl, M.A. Jakupec, W. Kandioller, B. K. Keppler, Inorg. Chim. Acta 513 (2020) 119919.
[42] J. Gomez, D. Sierra, C. Cardenas, F. Guzman, Curr. Org. Chem. 24 (2020) 2508–2523.
[43] Chin. Med. J. 92 (1979) 811–816.
[44] J. Krungkrai, S.R. Krungkrai, Asian Pac. J. Trop. Biomed. 6 (2016) 371–375.

[45] https://www.who.int/malaria/areas/treatment/overview/en/, 2020 (Date accessed: 10/11/2020).
[46] R. Ridley, Nature 415 (2002) 686–693.
[47] N. Vyas, B.A. Avery, M.A. Avery, C.M. Wyandt, Antimicrob. Agents Chemother. 46 (2002) 105.
[48] P.A. Buffet, I. Safeukui, G. Deplaine, V. Brousse, V. Prendki, M. Thellier, G. D. Turner, O. Mercereau-Puijalon, Blood 117 (2011) 381–392.
[49] P.A. Ndour, T.M. Lopera-Mesa, S.A.S. Diakité, S. Chiang, O. Mouri, C. Roussel, S. Jauréguiberry, S. Biligui, E. Kendjo, A. Claessens, L. Ciceron, D. Mazier, M. Thellier, M. Diakité, R.M. Fairhurst, P.A. Buffet, J. Infect. Dis. 211 (2014) 290–297.
[50] A. Robert, F. Benoit-Vical, C. Claparols, B. Meunier, Proc. Natl. Acad. Sci. U. S. A. 102 (2005) 13676.
[51] P.M. O'Neill, G.H. Posner, J. Med. Chem. 47 (2004) 2945–2964.
[52] A.E. Mercer, Curr. Opin. Drug. Discov. Dev. 12 (2009) 125–132.
[53] S. Krishna, A.-C. Uhlemann, R.K. Haynes, Drug Resist. Updat. 7 (2004) 233–244.
[54] L. Cui, X.-z. Su, Expert Rev. Anti-Infect. Ther. 7 (2009) 999–1013.
[55] O. Dechy-Cabaret, F. Benoit-Vical, J. Med. Chem. 55 (2012) 10328–10344.
[56] M.P. Crespo-Ortiz, M.Q. Wei, J. Biomed. Biotechnol. 2012 (2012) 247597.
[57] Y.K. Wong, C. Xu, K.A. Kalesh, Y. He, Q. Lin, W.S.F. Wong, H.-M. Shen, J. Wang, Med. Res. Rev. 37 (2017) 1492–1517.
[58] Y. Zhang, G. Xu, S. Zhang, D. Wang, P. Saravana Prabha, Z. Zuo, Nat. Prod. Bioprospect. 8 (2018) 303–319.
[59] X. Lu, T. Efferth, Semin. Cancer Biol. 68 (2021) 291–312.
[60] T.K. Kotammagari, S. Paul, G.K. Barik, M.K. Santra, A.K. Bhattacharya, Org. Biomol. Chem. 18 (2020) 2252–2263.
[61] R. An, B. Lin, S. Zhao, C. Cao, Y. Wang, X. Cheng, Y. Liu, M. Guo, H. Xu, Y. Wang, Z. Hou, C. Guo, Bioorg. Chem. 104 (2020) 104347.
[62] A. Çapcı, M.M. Lorion, H. Wang, N. Simon, M. Leidenberger, M.C. Borges Silva, D. R.M. Moreira, Y. Zhu, Y. Meng, J.Y. Chen, Y.M. Lee, O. Friedrich, B. Kappes, J. Wang, L. Ackermann, S.B. Tsogoeva, Angew. Chem. Int. Ed. 58 (2019) 13066–13079.
[63] K. Gogoi, G. Baishya, B. Saikia, N. Barua, C. Dohutia, A. Verma, A. Prakash, Asian Pac J Trop Med 12 (2019) 195–203.
[64] T. Fröhlich, F. Hahn, L. Belmudes, M. Leidenberger, O. Friedrich, B. Kappes, Y. Couté, M. Marschall, S.B. Tsogoeva, Chem. Eur. J. 24 (2018) 8103–8113.
[65] M. Navarro, W. Castro, C. Biot, Organometallics 31 (2012) 5715–5727.
[66] M. Henry, S. Briolant, A. Fontaine, J. Mosnier, E. Baret, R. Amalvict, T. Fusai, L. Fraisse, C. Rogier, B. Pradines, Antimicrob. Agents Chemother. 52 (2008) 2755–2759.
[67] C. Biot, F. Nosten, L. Fraisse, D. Ter-minassian, J. Khalife, D. Dive, Parasite 18 (2011) 207–214.
[68] C. Biot, G. Glorian, L.A. Maciejewski, J.S. Brocard, O. Domarle, G. Blampain, P. Millet, A.J. Georges, H. Abessolo, D. Dive, J. Lebibi, J. Med. Chem. 40 (1997) 3715.
[69] C. Biot, D. Taramelli, I. Forfar-Bares, L.A. Maciejewski, M. Boyce, G. Nowogrocki, J.S. Brocard, N. Basilico, P. Olliaro, T.J. Egan, Mol. Pharm. 2 (2005) 185–193.
[70] F. Dubar, C. Slomianny, J. Khalife, D. Dive, H. Kalamou, Y. Guérardel, P. Grellier, C. Biot, Angew. Chem. Int. Ed. 52 (2013) 7690–7693.
[71] G. Jaouen, A. Vessières, S. Top, Chem. Soc. Rev. 44 (2015) 8802–8817.
[72] C. Reiter, A. Çapcı Karagöz, T. Fröhlich, V. Klein, M. Zeino, K. Viertel, J. Held, B. Mordmüller, S. Emirdağ Öztürk, H. Anıl, T. Efferth, S.B. Tsogoeva, Eur. J. Inorg. Chem. 75 (2014) 403–412.
[73] C. Reiter, T. Fröhlich, M. Zeino, M. Marschall, H. Bahsi, M. Leidenberger, O. Friedrich, B. Kappes, F. Hampel, T. Efferth, S.B. Tsogoeva, Eur. J. Inorg. Chem. 97 (2015) 164–172.
[74] L.-i. Rylands, A. Welsh, K. Maepa, T. Stringer, D. Taylor, K. Chibale, G.S. Smith, Eur. J. Inorg. Chem. 161 (2019) 11–21.
[75] T. Stringer, M.A.S. Quintero, L. Wiesner, G.S. Smith, E. Nordlander, J. Inorg. Biochem. 191 (2019) 164–173.
[76] P. Chellan, K.M. Land, A. Shokar, A. Au, S.H. An, D. Taylor, P.J. Smith, T. Riedel, P. J. Dyson, K. Chibale, G.S. Smith, Dalton Trans. 43 (2014) 513–526.
[77] T. Stringer, D. Taylor, H. Guzgay, A. Shokar, A. Au, P.J. Smith, D.T. Hendricks, K. M. Land, T.J. Egan, G.S. Smith, Dalton Trans. 44 (2015) 14906–14917.
[78] P.M. Loiseau, N. Mbongo, C. Bories, Y. Boulard, D.G. Craciunescu, Parasite 7 (2000) 103–108.
[79] S.K. Singh, S. Joshi, A.R. Singh, J.K. Saxena, D.S. Pandey, Inorg. Chem. 46 (2007) 10869–10876.
[80] Y. Liu, Z. Liu, J. Shi, H. Chen, B. Mi, P. Li, P. Gong, Molecules 18 (2013) 2864.
[81] Z. Liu, A. Habtemariam, A.M. Pizarro, S.A. Fletcher, A. Kisova, O. Vrana, L. Salassa, P.C.A. Bruijnincx, G.J. Clarkson, V. Brabec, P.J. Sadler, J. Med. Chem. 54 (2011) 3011–3026.
[82] X. Deng, B. Wang, S. Xu, X. Zhou, L. Yang, Y. Li, Y. Hu, Y. Li, F. Zou, J. Mol. Cat. A: Chem. 184 (2002) 57–64.
[83] J. Tönnemann, J. Risse, Z. Grote, R. Scopelliti, K. Severin, Eur J Inorg, Chem 2013 (2013) 4558–4562.
[84] S. Duffy, V.M. Avery, Am. J. Trop. Med. Hyg. 86 (2012) 84–92.
[85] S. Duffy, V.M. Avery, Malar. J. 12 (2013) 408.
[86] S. Duffy, S. Loganathan, J.P. Holleran, V.M. Avery, Nat. Protoc. 11 (2016) 976–992.
[87] S.H. Adjalley, G.L. Johnston, T. Li, R.T. Eastman, E.H. Ekland, A.G. Eappen, A. Richman, B.K.L. Sim, M.C.S. Lee, S.L. Hoffman, D.A. Fidock, Proc. Natl. Acad. Sci. U. S. A. 108 (2011) E1214–E1223.
[88] R.A. Davis, M.S. Buchanan, S. Duffy, V.M. Avery, S.A. Charman, W.N. Charman, K. L. White, D.M. Shackleford, M.D. Edstein, K.T. Andrews, D. Camp, R.J. Quinn, J. Med. Chem. 55 (2012) 5851–5858.
[89] Richard K. Haynes, H.-W. Chan, M.-K. Cheung, W.-L. Lam, M.-K. Soo, H.-W. Tsang, A., Voerste and Ian D. Williams, Eur. J. Org. Chem. 2002 (2002) 113–132.
[90] S. Banerjee, P.J. Sadler, RSC Chem. Biol. 2 (2021) 12–29.
[91] T. Stringer, D.R. Melis, G.S. Smith, Dalton Trans. 48 (2019) 13143–13148.
[92] D.R. Melis, C.B. Barnett, L. Wiesner, E. Nordlander, G.S. Smith, Dalton Trans. 49 (2020) 11543–11555.
[93] E. Ekengard, K. Kumar, T. Fogeron, C. de Kock, P.J. Smith, M. Haukka, M. Monari, E. Nordlander, Dalton Trans. 45 (2016) 3905–3917.
[94] E. Ekengard, I. Bergare, J. Hansson, I. Doverbratt, M. Monari, B. Gordhan, B. Kana, C.D. Kock, P.J. Smith, E. Nordlander, J. Mex. Chem. Soc. 61 (2017) 158–166.
[95] P. Chellan, V.M. Avery, S. Duffy, J.A. Triccas, G. Nagalingam, C. Tam, L.W. Cheng, J. Liu, K.M. Land, G.J. Clarkson, I. Romero-Canelón, P.J. Sadler, Chem. Eur. J. 24 (2018) 10078–10090.
[96] Z. Liu, P.J. Sadler, Acc. Chem. Res. 47 (2014) 1174–1185.
[97] J.J. Soldevila-Barreda, A. Habtemariam, I. Romero-Canelón, P.J. Sadler, J. Inorg. Biochem. 153 (2015) 322–333.